Measurement of the Heat Load Imposed on the Reactor Vessel Depending on the Crust Layer in a Severe Accident

Joon-Soo Park, Hae-Kyun Park and Bum-Jin Chung*
Department of Nuclear Engineering, Kyung Hee University
#1732 Deogyeong-daero, Giheung-gu, Yongin-si, Gyeonggi-do, 17104, Korea
**Corresponding author*: *bjchung@khu.ac.kr*

1. Introduction

In an In-Vessel Retention and External Reactor Vessel Cooling (IVR-ERVC) situation, the molten corium in the oxide pool may be solidified and form a crust layer along the oxide layer boundary. This changes thermal boundary and geometrical condition of the oxide pool which may affect natural convection heat transfer of the oxide pool [1]. However, only a few studies [2,3] were performed regarding the crust layer. We measured the mean *Nu* imposed to reactor vessel and local heat flux and comparative analyses were performed between the crust free and crust conditions with a few different thicknesses depending on the decay heat.

2. Experimental set up

2.1 Experimental methodology

Heat and mass transfer systems are analogous. This means that the governing equations of two systems are mathematically the same. Thus, the heat transfer problems can be solved by the mass transfer experiments [4].

The limiting current technique, a method of measurement, is used by the mass transfer system and developed by several researchers [5–8], and this methodology is now well-established [9–11].

By using the mass transfer system, we could achieve high Ra'_H with compact test rigs, ideally isothermal cooling condition and uniform heat generation.

Because internal flow towards bottom of the test rig is formed in heat transfer, anode could simulate as cold wall in mass transfer. But, the current is not measured in anode [12]. Therefore, we performed the tests using the inverted test rigs against the gravity direction and simulated the same internal flow.

2.2 Phenomena modeling

To simulate the natural convection in the oxide pool, we assumed that the outer vessel wall is sustained as isothermal condition due to the ERVC and the temperature difference between inner and outer vessel wall was neglected to simplify modeling. Through these assumptions, the oxide pool boundary was simulated by an isothermal wall.

Thickness of the crust layer, Δx, is determined by the heat balance, $q'' = -k(\Delta T/\Delta x)$. The heat balance equations [13] and geometrical and thermodynamic properties [13–15] were employed to estimate the crust layer thickness.

The temperature difference in the system is reduced by the crust layer. When the crust layer is formed, the temperature of the oxide pool boundary is changed into the melting temperature of the crust layer. In the mass transfer system, the temperature difference was replaced with the concentration difference. *Da* in the system was also changed by analogy. In the heat transfer system, the *Da* ratio ($\Delta T_2/\Delta T_1$) was 0.130. In order to maintain the ratio, the working fluid concentrations were determined as 0.026 M for with curst and 0.2 M for without crust.

Table I listed the test matrix. It was confirmed that a semi-circular test rig with 0.1 m height can achieve Ra'_H of ~ 10^{15} in previous studies of our research group [9–11,16–21]. Based on this, the thicknesses of the crust layer were downscaled in mass transfer system.

Table I: Test matrix

Crust formation	Thickness (m)	Ra'_H	*Pr*
With crust	N/A	9.51×10^{14}	2283
Without crust	0.003	6.23×10^{13}	1979
	0.01	4.79×10^{13}	
	0.03	1.63×10^{13}	
	0.05	3.97×10^{12}	

Figure 1 presents the test rigs, mass transfer experimental rig for a 2-D oxide pool with crust layer (MassTER-OP2(CL)), which radius is 0.1 m. The width is 0.04 m, which is enough to neglect the effect of the side wall [22]. The copper cathodes were located along the inner surface. To check the influence of insulation layers among piecewise electrodes, halves of the inner surfaces consisted of a single electrode and the other halves consisted of piecewise electrodes for the local currents measurement. The curved surface consisted of nine piecewise electrodes, and eight along the top plate. To simulate the internal heat source, copper anodes were attached at both sides. Copper sulfate-sulfuric acid ($CuSO_4$-H_2SO_4) solution was used as a working fluid.

Figure 2 presents the experimental circuit. A power supply (K1810 of Vüpower) and data acquisition system (NI-9225, NI-9227 of National Instruments) was used.

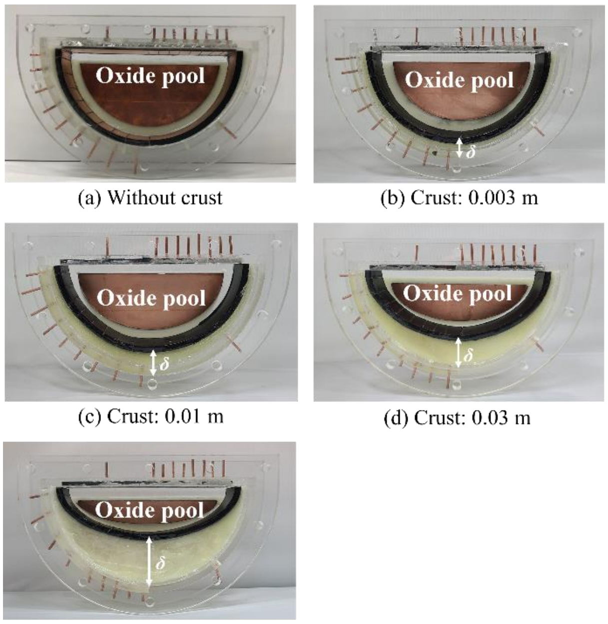

(a) Without crust (b) Crust: 0.003 m
(c) Crust: 0.01 m (d) Crust: 0.03 m
(e) Crust: 0.05 m

Fig. 1. Test rigs.

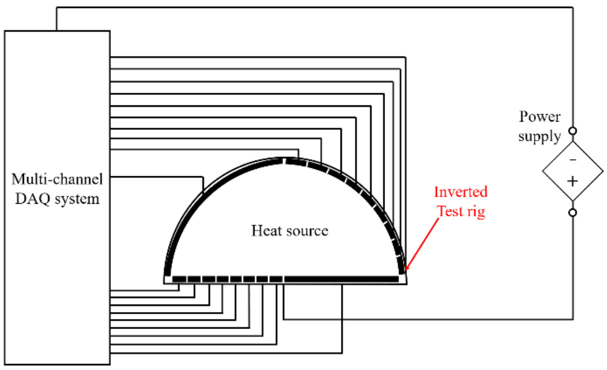

Fig. 2. Experimental circuit.

3. Results and Discussion

Figure 3(a) presents the local heat transfer coefficient (h_{loc}) measured along the curved surface for both conditions. The h_{loc} values in without crust layer condition were greater than those in with crust layer condition because the crust layer works as the thermal insulator.

Figure 3(b) shows the h_{loc} values of the top plate. The h_{loc} values in without crust layer condition were greater than those in with crust layer condition as more heat is imposed to top plate because of insulation effect of the crust layer. In without crust condition, the h_{loc} values had a peak at the center. The rising plume from the bottom of the curved surface improved the h_{loc} at the center of the top plate. Meanwhile, monotonic shape of h_{loc} was observed in the with crust condition. This seems to be induced by the thermal boundary condition. In with crust layer condition, the temperature difference is decreased and Ra'_H decreased from 9.51×10^{14} to 6.23×10^{13}. Hence, the buoyancy of the rising plume was reduced and a side flow was generated before it arrives at the top plate in with crust condition. In all cases, the h_{loc} at the edge of the top plate showed very low heat transfer because the stagnant flow was generated.

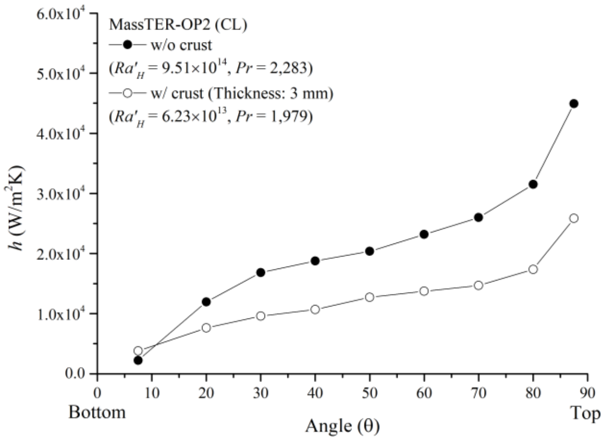

(a) Local heat transfer coefficient at the curved surface

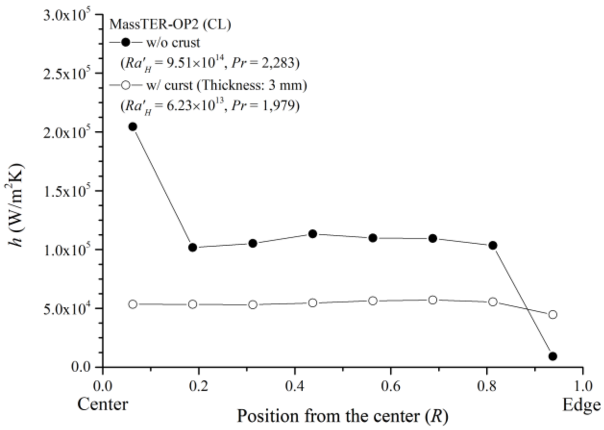

(b) Local heat transfer coefficient at the top plate

Fig. 3. Comparison of local heat transfer coefficient according to the crust existence.

Figure 4 presents the h_{loc} measured at the curved surface and top plate according to crust thickness. The h_{loc} values measured at the curved surface is reduced as the crust layer became thicker, as shown in Fig. 4(a). Because increase in curst thickness leads to decrease in Ra'_H, which leads to decrease in h_{loc}. Fig. 4(b) presents that the h_{loc} values measured at the top plate increased when the crust thickness increased as the downward cooling was decreased.

A comprehensive analysis was performed by comparing the h_{loc} values in Figs. 3 and 4 shows that the heat loads imposed on the reactor vessel are influenced by the crust layer. That the influence of the variation due to thermal boundary condition is more pronounced than that of the variation due to crust thickness.

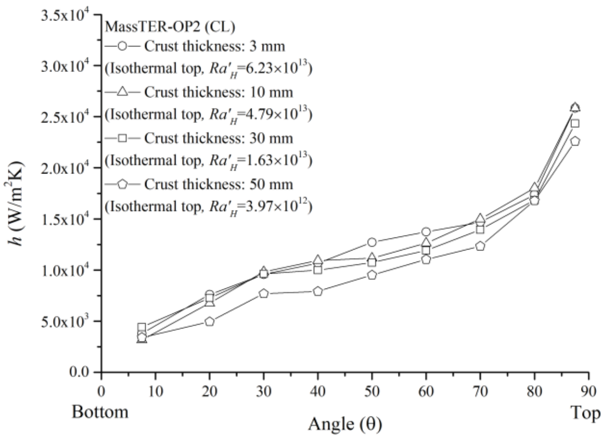

(a) Local heat transfer coefficient at the curved surface

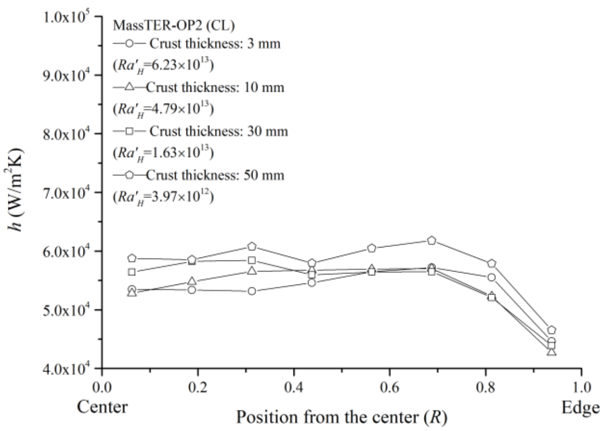

(b) Local heat transfer coefficient at the top plate

Fig. 4. Comparison of local heat transfer coefficient according to the thickness of crust layer.

4. Conclusions

The natural convection heat transfer of the oxide pool when the crust layer was formed was simulated. Before the design of experiments, we conducted modeling for the crust situation. This is the originality of this study. We investigated the crust layer influence on the heat load imposed on reactor vessel in an IVR condition. The range of Ra'_H was $10^{12} – 10^{15}$.

When the crust layer is formed, thermal boundary condition of oxide pool is varied from the boiling temperature of the external coolant to the melting temperature of the oxide pool. The temperature difference of the system was decreased and the driving force was weakened.

The experimental results presented that the crust layer disturbed the heat transfer at the oxide pool as it works as the thermal insulator. The effect of crust layer thickness on the local heat transfer was small compared to effect caused by the formation of the crust layer. Thus the effect of the crust layer due to the variation of the thermal boundary condition was greater than the effect due to the crust thickness.

NOMENCLATURE

Da	Damkőhler number ($q'''H^2/k\Delta T$)
h	Heat transfer coefficient [$W/m^2 \cdot K$]
h_{loc}	Local heat transfer coefficient [$W/m^2 \cdot K$]
H	Oxide pool height [m]
k	Thermal conductivity [$W/m \cdot K$]
Pr	Prandtl number (ν/α)
q''	Heat flux [W/m^2]
q'''	Volumetric heat generation rate [W/m^3]
R	Position from the center
Ra_H	Rayleigh number ($g\beta\Delta TH^3/\alpha\nu$)
Ra'_H	Modified Rayleigh number ($Ra_H Da$)
ΔT	Temperature difference of the system [K]
ΔT_1	Temperature difference of the system in without crust condition [K]
ΔT_2	Temperature difference of the system in with crust condition [K]
Δx	Crust layer thickness [m]

Greek symbols

α	Thermal diffusivity
β	Volume expansion coefficient [$1/K$]
δ	Crust layer thickness of test rigs [m]
θ	Angle [^{o}]
ν	Kinematic viscosity [m^2/s]
ρ	Density [kg/m^3]

ACKNOWLEDGEMENT

This study was sponsored by the Ministry of Science and ICT and was supported by Nuclear Research & Development program grant funded by the National Research Foundation (NRF) (Grant code: 2017M2A8A4015283).

This work was also supported by “Human Resources Program in Energy Technology” of the Korea Institute of Energy Technology Evaluation and Planning (KETEP), granted financial resource from the Ministry of Trade, Industry & Energy, Republic of Korea (No. 20184030202170).

REFERENCES

[1] T. H. Fan, F. B. Cheung, Modeling of Transient Turbulent Natural Convection in a Melt Layer with Solidification, Journal of Heat Transfer, Vol. 119, pp. 544–552, 1997.
[2] M. Helle, O. Kymäläinen, H. Tuomisto, Experimental Data on Heat Flux Distribution from a Volumetrically Heated Pool with Frozen Boundaries, IVO Power Engineering Ltd., 1998.
[3] Y. P. Zhang, L. T. Zhang, Y. K. Zhou, W. X. Tian, S. Z. Qiu, G. H. Su, B. Zhao, T. D. Yuan, R. B. Ma, Natural Convection Heat Transfer Test for In-Vessel Retention at Prototypic Rayleigh Numbers – Results of COPRA experiments, Progress in Nuclear Energy, Vol. 86, pp. 80–86, 2016.
[4] A. Bejan, Convection Heat Transfer, Third ed, New York: John Wiley & Sons, INC, pp. 96-97, 173-179, 197-200, 512-516, 2006.
[5] V. G. Levich, Physicochemical Hydrodynamics, Prentice-Hall, Englewood Cliffs, New Jersey, 1962.

[6] J. N. Agar, Diffusion and Convection at Electrodes, Discuss. Faraday Soc. Vol. 26, pp. 27-37, 1947.
[7] C. W. Tobias, R. G. Hickman, Ionic Mass Transfer by Combined Free and Forced Convection, International Journal of Research in Physical Chemistry and Chemical Physics, Vol. 229, pp. 145-166, 1965.
[8] E. J. Fenech, C. W. Tobias, Mass transfer by free convection at horizontal electrodes, Electrochimica Acta, Vol. 2, pp. 311-325, 1960.
[9] J. W. Bae, B. J. Chung, Comparison of 2-D and 3-D IVR experiments for oxide layer in the three-layer configuration, Nuclear Engineering and Technology, Vol. 52, pp. 2499–2510, 2020.
[10] H. K. Park, S. H. Kim, B. J. Chung, Variation in the angular heat flux of the oxide pool with Rayleigh number, Annals of Nuclear Energy, Vol. 170, pp. 128–135, 2017.
[11] Kim and Chung, Heat Load Imposed on Reactor Vessel During In-Vessel Retention of Core Melts, Nuclear Engineering and Design, Vol. 308, pp. 1–8, 2016
[12] Y. Konishi, Y. Nakamura, Y. Fukunaka, K. Tsukada, K. Hanasaki, Anodic Dissolusion Phenomena Accompanying Supersaturation of Copper Sulfate Along a Vertical Plane Copper Anode, Electrochimica Acta, Vol. 48, pp. 2615–2624, 2003.
[13] H. Esmaili, M. K. Rahbar, Analysis of In-Vessel Retention and Ex-Vessel Fuel Coolant Interaction for AP1000, U.S. NRC, NUREG/CR-6849, ERI/NRC-04-201, 2004.
[14] J. L. Rempe, K. Y. Suh, F. B. Cheung, S. B. Kim, In-Vessel Retention Strategy for High Power Reactor, Final report, INEEL/EXT-04-02561, 2005.
[15] J. H. Jung, S. M. An, K. S. Ha, H. Y. Kim, Evaluation of Heat-Flux Distribution at the Inner and Outer Reactor Vessel Walls Under the In-Vessel Retention Through External Reactor Vessel Cooling Condition, Nuclear Engineering Technology, Vol. 47, pp. 66–73, 2015.
[16] H. K. Park, B. J. Chung, Mass Transfer Experiments for the Heat Load During In-Vessel Retention of Core Melt, Nuclear Engineering and Technology, Vol. 48, pp. 906–914, 2016.
[17] S. H. Kim, H. K. Park, B. J. Chung, Two- and Three-Dimensional Experiments for Oxide Pool in In-Vessel Retention of Core Melts, Nuclear Engineering and Technology, Vol. 49, pp. 1405–1413, 2017.
[18] S. H. Kim, H. K. Park, B. J. Chung, Natural Convection of the Oxide Pool in a Three-Layer Configuration of Core Melts, Nuclear Engineering and Design, Vol. 317, pp. 100–109, 2017.
[19] H. K. Park, S. H. Kim, B. J. Chung, Natural Convection of Melted Core at the Bottom of Nuclear Reactor Vessel in a Severe Accident, International Journal of Energy Research, Vol. 42, pp. 303–313, 2018.
[20] S. H. Kim, B. J. Chung, Mass Transfer Experiments on the Natural Convection Heat Transfer of the Oxide Pool in a Three-Layer Configuration, Progress in Nuclear Energy, Vol. 106, pp. 11–19, 2018.
[21] J. W. Bae, B. J. Chung, Development of Multi-Cell Flows in the Three-Layered Configuration of Oxide Layer and Their Influence on the Reactor Vessel Heating, Nuclear Engineering and Technology, Vol. 51, pp. 996–1007, 2019.
[22] T. N. Dinh, R. R. Nourgaliev, B. R. Sehgal, On Heat Transfer Characteristics of Real and Simulant Melt Pool Experiments, Nuclear Engineering and Design, Vol. 169, pp. 151–164, 1997.